Eur. Phys. J. D (2018) 72: 130
https://doi.org/10.1140/epjd/e2018-90150-7

THE EUROPEAN PHYSICAL JOURNAL D

Regular Article

Helium nanodroplets doped with copper and water*

Stefan Raggl[1], Norbert Gitzl[1], Paul Martini[1], Paul Scheier[1,a], and Olof Echt[1,2,b]

[1] Institut für Ionenphysik und Angewandte Physik, Universität Innsbruck, Technikerstr. 25, 6020 Innsbruck, Austria
[2] Physics Department, University of New Hampshire, Durham NH 03824, USA

Received 2 April 2018 / Received in final form 10 May 2018
Published online 12 July 2018

Abstract. Copper nanoparticles are promising, low-cost candidates for the catalytic splitting of water and production of hydrogen gas. The present gas-phase study, based on the synthesis of copper-water complexes in ultracold helium nanodroplets followed by electron ionization, attempts to find evidence for dissociative water adsorption and H_2 formation. Mass spectra show that H_2O–Cu complexes containing dozens of copper and water molecules can be formed in the helium droplets. However, ions that would signal the production and escape of H_2, such as $(H_2O)_{n-2}(OH)_2Cu_m^+$ or the isobaric $(H_2O)_{n-1}OCu_m^+$, could not be detected. We do observe an interesting anomaly though: While the abundance of stoichiometric $(H_2O)_nCu_m^+$ ions generally exceeds that of protonated or dehydrogenated ions, the trend is reversed for $(H_2O)OHCu_2^+$ and $(H_2O)_2OHCu_2^+$; these ions are more abundant than $(H_2O)_2Cu_2^+$ and $(H_2O)_3Cu_2^+$, respectively. Moreover, $(H_2O)_2OHCu_2^+$ is much more abundant than other ions in the $(H_2O)_{n-1}OHCu_2^+$ series. A byproduct of our experiment is the observation of enhanced stability of He_6Cu^+, $He_{12}Cu^+$, $He_{24}Cu^+$, and $He_2Cu_2^+$.

1 Introduction

Copper nanoparticles dispersed in water or in the form of coatings have a range of promising uses, including lubrication, ink jet printing, as luminescent probes, exploiting their antimicrobial and antifungal activity, and in fuel cells [1–6]. Thermodynamic data predict that water splitting at monocrystalline copper surfaces does not produce significant amounts of molecular hydrogen but the evolution of hydrogen gas from oxygen-free water in contact with copper surfaces has been observed [7].

Theoretical studies of the reaction of water with surfaces of crystalline copper have been reported by Johansson et al. [8] and Lousada et al. [9]. At the low-density [110] surface, dissociation of adsorbed H_2O is spontaneous; it has a lower activation energy than at the higher-density [100] or [111] surface. The activation energy decreases with increasing water coverage. The autocatalytic dissociation of water on the Cu[110] surface has, indeed, been identified by photoelectron spectroscopy at near-ambient conditions [10].

Johansson et al. have suggested that water oxidizes Cu[100] until the surface is saturated with hydroxyl groups, and that H_2 forms by direct combination of hydrogen atoms at the surface [8]. Lousada et al. conclude that a monolayer of molecularly adsorbed H_2O at Cu[110] spontaneously converts to $\frac{1}{2}$ monolayer of OH plus $\frac{1}{2}$ monolayer of H_2O accompanied by the release of hydrogen gas [9].

In industrial applications the surface of a copper catalyst is not crystalline. Some catalytic reactions may be promoted by atoms or small clusters of copper [11,12]. Huseyinova et al. have reported the synthesis of surfactant-free, nearly mono-disperse Cu_5 clusters in water that are stable to UV irradiation, elevated temperature, and a wide range of pH [13]. Their catalytic activity has not yet been measured, but several theoretical studies of water dissociation on Cu_7 have been reported [14–16]. Cu_7 represents a prototypical cluster because most DFT-based calculations predict that the ground-state structures of copper clusters Cu_m are planar for $3 \leq m \leq 6$ while Cu_7 forms a pentagonal bipyramid [17].

Based on a DFT approach, Chen et al. conclude that the main driving force for the adsorption of H_2O at Cu_7 is the overlap between the *p*-orbital of O occupied by the lone pair and the 3*d* orbitals of Cu [14]. Dissociative adsorption of a single H_2O to form OH and H is exothermic with a moderately high barrier. The reaction can be catalyzed by another H_2O via hydrogen bonding. At high water coverage, the reaction becomes much more favorable both thermochemically and kinetically. Two OH species can react to form an O adatom plus H_2O.

A DFT study by Stenlid et al. focuses on the formation of molecular hydrogen upon reaction of H_2O with Cu_7, and the role of large water coverage [15]. The authors conclude that the reaction of an adsorbed H atom with H_2O yielding H_2+OH is much faster than the direct

* Contribution to the Topical Issue "Atomic Cluster Collisions", edited by Alexey Verkhovtsev, Andrey V. Solov'yov, Germán Rojas-Lorenzo, and Jesús Rubayo Soneira.

[a] e-mail: paul.scheier@uibk.ac.at
[b] e-mail: olof.echt@unh.edu

combination of two H atoms. Under atmospheric H_2 pressure the thermodynamically most favored reaction is $Cu_7 + 8\ H_2O \rightarrow (OH)_8Cu_7 + 4\ H_2$.

The reports discussed so far involve neutral complexes. Water splitting in ionic systems is of interest, too, because in the condensed phase metallic clusters may be charged [16]. Furthermore, the influence of the charge will likely decrease as the size of the copper cluster increases.

Several experimental studies of ionic copper-water complexes in the gas phase have been reported; most are restricted to atomic Cu^+ or Cu^{2+}. Holland and Castleman have used high-pressure mass spectrometry to determine thermochemical properties of $(H_2O)_nCu^+$ for $n = 3, 4, 5$ [18]. Michl and coworkers as well as Armentrout and coworkers measured dissociation energies D_n (or sequential binding energies) of $(H_2O)_nCu^+$ for $1 \leq n \leq 4$ by collision-induced dissociation [19,20]. $(H_2O)_2Cu^+$ is remarkably stable; it's dissociation energy (1.7 eV) exceeds that of $(H_2O)Cu^+$ by about 0.2 eV [19]. Several theoretical studies have shown that Cu^+ is, indeed, two-fold coordinated; the oxygen atoms of the first two H_2O bind to opposite sides of Cu^+ [21–25]. The interaction is nearly evenly divided among electrostatic, polarization, and charge transfer; the Cu Mulliken charge is only $+0.85\ e$ [25]. Properties of $(H_2O)_nCu^+$ have also been explored by vibrational spectroscopy [26–28]. $(H_2O)_nOHCu^+$ complexes have been characterized by vibrational spectroscopy and collision-induced dissociation [29–32] as well as theoretical modeling [31].

In contrast to these numerous studies of $(H_2O)_nCu^+$ and $(H_2O)_nOHCu^+$, we are aware of only two gas-phase studies that mention complexes containing more than one copper atom. Michl and coworkers observed $(H_2O)_nHCu_2^+$, $(H_2O)_{n-1}OHCu_2^+$, and $(H_2O)_{n-1}OCu_2^+$ but no $(H_2O)_nCu_2^+$ upon fast-atom bombardment of frosted copper surfaces; unfortunately they did not quantify the yield of these ions nor the range of n values [19] (Here the chemical formulas are written such that the subscript n specifies the number of oxygen atoms; they do not necessarily convey structural information). Stace and coworkers used a pulsed-arc cluster source; they observed predominantly $(H_2O)_nHCu_2^+$ and $(H_2O)_nH_2Cu_2^+$ $(n \leq 10)$, $(H_2O)_{n-1}OHCu_3^+$, and $(H_2O)_{n-1}OCu_3^+$ [33]. Pure hydrated Cu_2^+ and Cu_3^+ was noticeably absent, with the exception of $H_2OCu_3^+$.

In the present work we have synthesized neutral copper-water complexes by successively doping cold (0.37 K), superfluid helium nanodroplets with copper atoms and water molecules; the droplets are then ionized by electrons. The composition of the most prominent ions depends on the partial pressures in the pickup cell. We observe ions containing several copper atoms and several dozen water molecules. The stoichiometries of the most prominent ions are $(H_2O)_nCu_m^+$, $(H_2O)_{n-1}OHCu_m^+$, and $(H_2O)_nHCu_m^+$. Surprisingly, $(H_2O)_nCu_m^+$ ions which were essentially absent from previous work [19,33] form the most abundant ion series, with just one exception: $(H_2O)_2OHCu_2^+$ is more abundant than $(H_2O)_3Cu_2^+$. We have not been able to clearly identify $(H_2O)_{n-1}OCu_m^+$ which could indicate H_2 formation, but the mass spectra are highly congested.

As a by-product, we have recorded mass spectra of helium droplets doped with copper but no water, leading to the formation of $He_nCu_m^+$. The He_nCu^+ series features local maxima at $n = 6$, 12 and 24. Maxima at $n = 6$ and 12 have previously been observed for Ar_nCu^+ and Ne_nCu^+, respectively, and rationalized by DFT calculations [34]. The significance of those observations for our results will be discussed.

2 Experiment

Helium nanodroplets were produced by expanding helium (Linde, purity 99.9999%) at a stagnation pressure of 25 bar through a 5 μm nozzle, cooled by a closed-cycle cryostat to between 9 and 10 K, into vacuum. Droplets formed at these conditions contain roughly 10^6 atoms. The exact temperatures and estimated [35] average numbers of helium atoms in the droplets will be specified in the Result section.

The expanding beam was skimmed by a 0.8 mm conical skimmer located 8 mm downstream from the nozzle and traversed an 8 cm long, differentially pumped pick-up cell filled with copper vapor produced in a resistively heated oven. The temperature of the copper oven could not be measured directly; it was adjusted in order to obtain the optimal conditions for formation of either $He_nCu_m^+$ or $(H_2O)_nCu_m^+$ cluster ions. Water vapor was introduced into a second differentially pumped pickup chamber from an external water reservoir.

The beam of doped helium droplets was collimated and crossed by an electron beam with a nominal energy of 70–80 eV. Cations were accelerated into the extraction region of a reflectron time-of-flight mass spectrometer (Tofwerk AG, model HTOF) with an effective mass resolution $m/\Delta m = 3000$ (Δm = full-width-at-half-maximum). The base pressure in the mass spectrometer was 10^{-5} Pa. Ions were extracted at 90° into the field-free region of the spectrometer by a pulsed voltage. At the end of the field-free region they entered a two-stage reflectron which reflected them towards a microchannel plate detector operated in single ion counting mode. Further experimental details have been provided elsewhere [36].

Mass spectra were evaluated by means of a custom-designed software [37]. The abundance of ions is derived from the mass spectra by a matrix method. The routine includes automatic fitting of a custom peak shape to the mass peaks and subtraction of background by fitting a spline to the background level of the raw data. Hydrogen and helium are very nearly monoisotopic (the natural abundance of deuterium is 0.0115%; that of ^{3}He is 0.000137%) but copper has two naturally occurring isotopes, ^{63}Cu (mass 62.9296 u, natural abundance 69.17%) and ^{65}Cu (64.9278 u, 30.83%).

3 Experimental results

Figure 1a displays a mass spectrum of helium nanodroplets doped with copper but no water, ionized

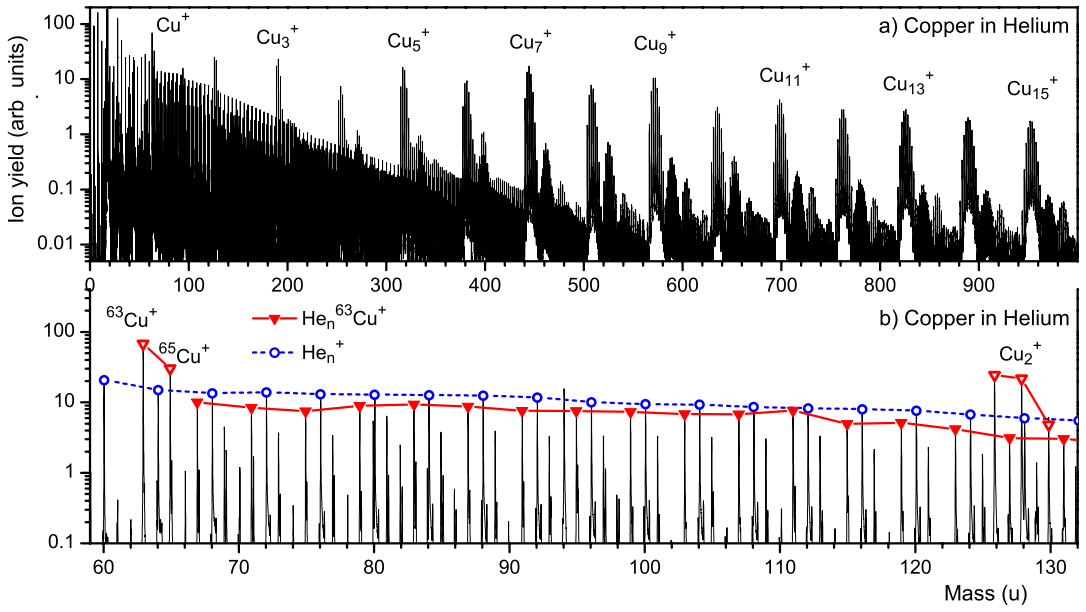

Fig. 1. Panel (a) shows a mass spectrum of helium droplets (estimated average size 5×10^6 atoms) doped with copper but no water. The most prominent series of mass peaks are due to He_n^+ and Cu_m^+. Local variations in the ion yield of Cu_m^+ reflect variations in cluster stability due to electronic shell effects. Panel (b) displays a section of the spectrum; mass peaks due to He_n^+ (open circles) and $He_n{}^{63}Cu_m^+$ (full triangles) are flagged. Open triangles mark the two isotopes of Cu^+ and the three isotopologues of Cu_2^+.

at an electron energy of 71 eV. Helium was expanded at 25 bar through a 5 μm nozzle cooled to 9.25 K. At these conditions, the estimated average number of helium atoms in a droplet is 5×10^6 helium atoms [35].

The most prominent mass peaks in Figure 1a are due to Cu_m^+, $m \leq 15$. Complexes of Cu_m^+ with a water molecule (due to a water contamination) become apparent for $m \geq 3$; for $m \geq 7$ complexes with two water molecules appear as well. Another minor contamination is assigned to PH^+ (mass 31.982 u); it appears when the copper oven is heated. The mass peak of PH^+ is distinct from that of O_2^+ (31.990 u) but $PHCu_m^+$ and $O_2Cu_m^+$ cannot be distinguished for $m \geq 1$.

Figure 1b zooms into the mass region between Cu^+ and Cu_2^+. The two naturally occurring isotopes of copper (^{63}Cu and ^{65}Cu) and the three isotopologues of Cu_2 are marked by open triangles. Solid triangles connected by a solid line mark mass peaks due to $He_n{}^{63}Cu^+$; they are nearly as intense as pure He_n^+ ions (open dots connected by a dotted line).

Figure 2 displays the ion abundance of He_nCu^+ and $He_nCu_2^+$ deduced from the mass spectrum in Figure 1 with a custom-designed software [37]. Uncertainties are reported by the software; a few statistically significant anomalies are marked. Some error bars are very large as a result of mass spectral coincidence with potential contaminants. For example, $He_4{}^{63}Cu^+$ and $He_4{}^{65}Cu^+$ cannot be distinguished from $O^{63}Cu^+$ and $H_2O^{63}Cu^+$, respectively (the relative mass differences are $\Delta m/m \leq 2 \times 10^{-4}$).

A mass spectrum of helium droplets doped with copper and water is presented in Figure 3. Data were recorded with a helium stagnation pressure of 25 bar, nozzle temperature 9.65 K, estimated droplet size 5×10^5 atoms,

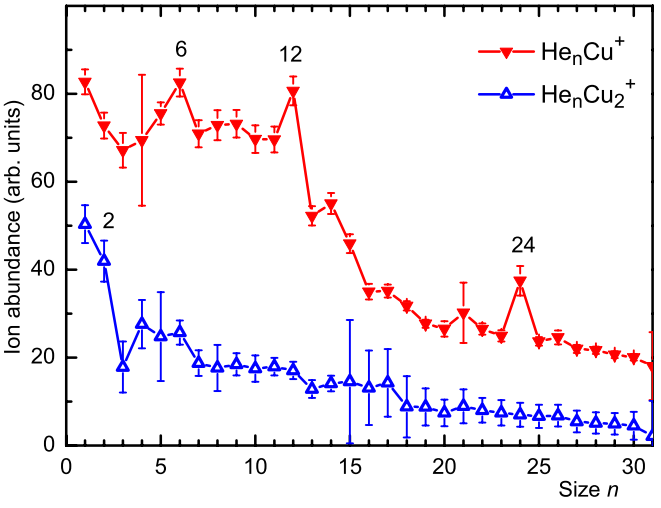

Fig. 2. The ion abundance of He_nCu^+ and $He_nCu_2^+$ deduced from the mass spectrum displayed in Figure 1.

electron energy 80 eV. The total pressure (mostly water) in the pickup cell was 1×10^{-5} mbar. The temperature of the copper oven was about the same as used to record the spectrum in Figure 1. The most prominent mass peaks in Figure 3 are due to He_n^+ and, above about 150 u, $(H_2O)_nH^+$ (for the sake of consistency, we write all chemical formulas such that the subscript n specifies the number of oxygen atoms in a complex; they are not meant to convey structural information).

Figure 4 zooms into a section of the spectrum. Mass peaks due to $(H_2O)_n{}^{63}Cu^+$ are marked by solid triangles,

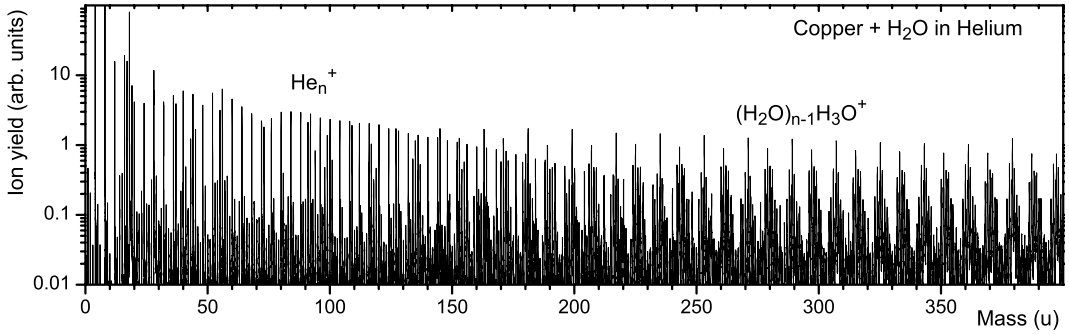

Fig. 3. Mass spectrum of helium droplets (estimated average size 5×10^5 atoms) doped with copper and water. The most prominent ion series below 150 u is due to He_n^+; at higher masses pure protonated water clusters dominate.

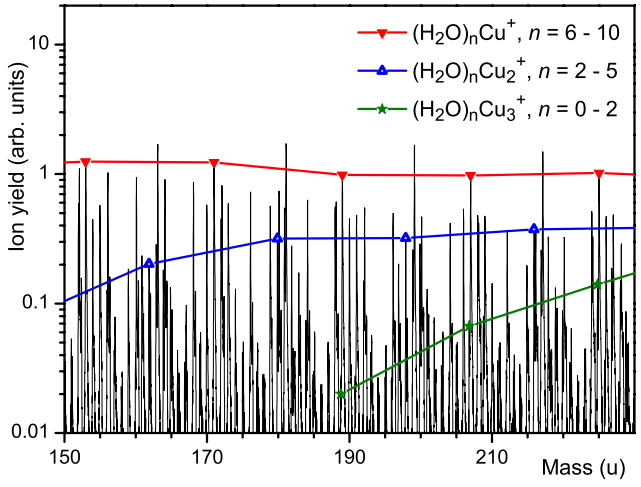

Fig. 4. A section of the spectrum displayed in Figure 3. Mass peaks due to $(H_2O)_n{}^{63}Cu^+$, $(H_2O)_n{}^{63}Cu_2{}^+$, and $(H_2O)_n{}^{63}Cu_3{}^+$ are marked. The most prominent mass peaks (not marked) are due to protonated water clusters.

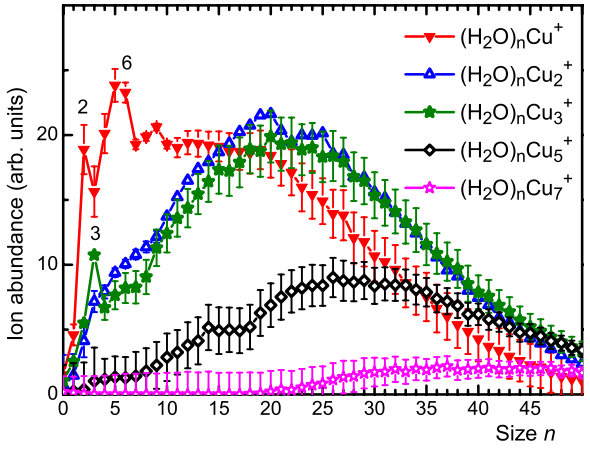

Fig. 5. The ion abundance of $(H_2O)_nCu_m{}^+$ versus n for $m = 1, 2, 3, 5, 7$, extracted from the mass spectrum displayed in Figure 3.

peaks due to $(H_2O)_n{}^{63}Cu_2{}^+$ by open triangles, peaks due to $(H_2O)_n{}^{63}Cu_3{}^+$ by stars.

The ion abundance of $(H_2O)_nCu_m{}^+$ extracted from this spectrum for $1 \leq m \leq 7$ is displayed in Figure 5. For clarity, data for $m = 4$ and 6 have been omitted; they smoothly interpolate between distributions of their next smaller and larger sibblings. Strong, statistically significant local maxima in the distributions at $(H_2O)_2Cu^+$ and $(H_2O)_3Cu_3{}^+$ and an abrupt drop beyond $(H_2O)_6Cu^+$ are marked.

Figure 6 compiles the ion abundances of $(H_2O)_nCu_m{}^+$, $(H_2O)_nHCu_m{}^+$, and $(H_2O)_{n-1}OHCu_m{}^+$ cluster ions for $m = 1$, 2, 3 (panels (a), (b), and (c), respectively). Stoichiometric $(H_2O)_nCu_m{}^+$ ions are nearly always more abundant than the protonated or dehydrogenated ions with the same (m,n) values, but $(H_2O)OHCu_2{}^+$ and $(H_2O)_2OHCu_2{}^+$ are more abundant than $(H_2O)_2Cu_2{}^+$ and $(H_2O)_3Cu_2{}^+$, respectively. Furthermore, $(H_2O)_2OHCu_2{}^+$ (i.e. $n = 3$) forms a pronounced local maximum in the series of dehydrogenated ions. The local anomalies marked in panels (a) ($(H_2O)_2Cu^+$ and $(H_2O)_6Cu^+$)) and (c) ($(H_2O)_3Cu_3{}^+$) were already mentioned in the context of Figure 5.

4 Discussion

4.1 Copper-water complexes

The main motivation for the present work is the identification of ions that might signal the splitting of water on the surface of copper cluster ions. Several theoretical studies suggest that hydration of Cu_7 may lead to the evolution of molecular H_2 [14–16]. Water splitting can be catalyzed by another H_2O via hydrogen bonding. Water coverage beyond the first monolayer favors the reaction, thermochemically as well as kinetically [16].

These studies pertain to neutral clusters containing seven atoms (Cu_7 is commonly chosen because it is the smallest three-dimensional cluster, but the reaction energetics and kinetics may be similar for other small clusters [14]). In our experiment, neutral water-copper complexes are synthesized in superfluid helium nanodroplet by successive capture of H_2O and Cu, in random order. This is a statistical process which leads to a broad distribution in the size distribution of $(H_2O)_xCu_y$, amplified by the considerable size range of the helium nanodroplets. The mass spectra show that x may be as large as ≈50, and y may exceed ≈20. Presumably there is no lower limit to the values of x and y.

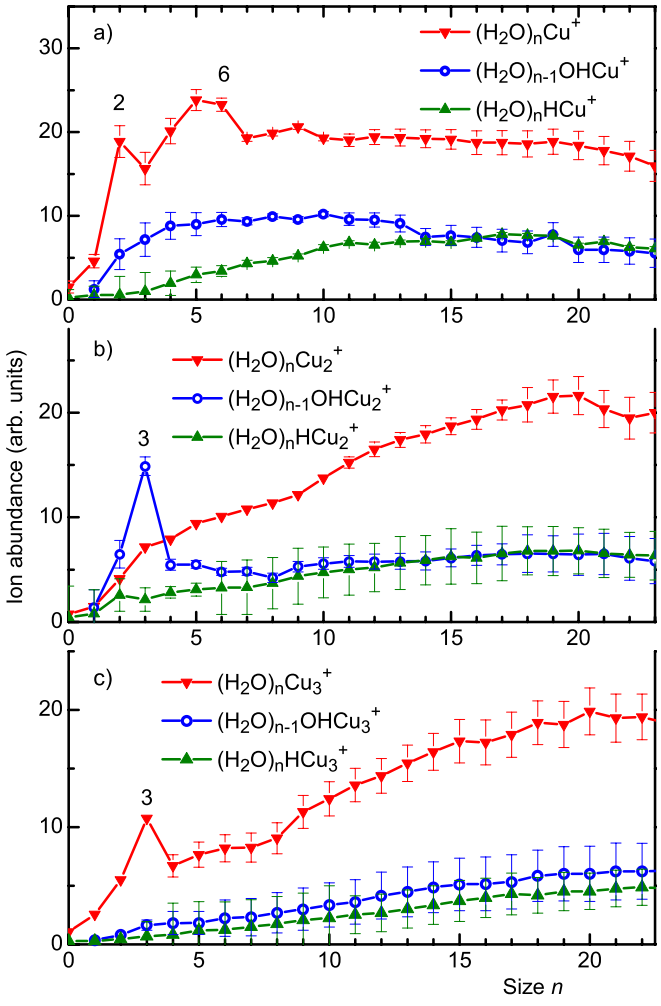

Fig. 6. The ion abundance of $(H_2O)_nCu_m^+$ together with that of dehydrogenated and protonated ions, for $m = 1, 2, 3$ (panels (a), (b), and (c), respectively). Values of n at which strong local anomalies occur are marked.

Water splitting is unlikely to occur during synthesis of $(H_2O)_xCu_y$ in a helium droplet because the droplet temperature is only 0.37 K; the energy released upon aggregation is rapidly removed by evaporation of helium atoms (which costs about 0.6 meV per atom). However, ionization of the dopant is an indirect process which starts with the formation of He^+ and resonant hole hopping, or of electronically excited, highly mobile He^{*-} [38]. Formation of He^+ requires about 24.6 eV while the ionization energy of Cu is 7.73 eV; the difference will be released upon charge transfer between He^+ and Cu. The excess energy would be a few eV smaller if ionization involves He^{*-}.[1] On the other hand, the excess energy would be a few eV larger for large copper clusters whose ionization energies converge towards the copper work function (≈5 eV). Thus an excess energy of 17 eV, give or take a few eV, will be released upon ionization of the dopant.

[1] Furthermore, the emitted electrons could possibly carry away a large fraction of the excess energy.

Electron ionization mass spectra of clusters embedded in helium nanodroplets do, in fact, indicate extensive intra- and intermolecular fragmentation. Often the spectra are very similar to mass spectra recorded by direct electron ionization of bare clusters at commonly used (70 eV) energies. For example, electron ionization of water clusters embedded in helium as well as electron ionization of bare water clusters result in predominantly protonated water cluster ions, $(H_2O)_nH^+$, and an abrupt drop in the ion abundance at $n = 21$ [39,40].

Furthermore, the mass spectrum in Figure 1 provides direct evidence for ionization-induced dissociation. Although the size distribution of neutral clusters is smooth because of the statistical nature of the capture process, the measured abundance distribution of Cu_m^+ closely tracks the size dependence of their dissociation energies, with the electronically closed-shell Cu_3^+ and Cu_9^+ being much more stable than Cu_4^+ and Cu_{10}^+, respectively [41]. The evaporative model explains why local anomalies in cluster ion abundance distributions reflect anomalies in their relative dissociation energies, provided each cluster ion has lost at least one atom before the distribution is being measured [42,43]. The dissociation energies of Cu_3^+ and Cu_9^+ are 2.83 and 3.66 eV [41] proving that ample energy becomes available when copper clusters embedded in helium are ionized by electron impact.

Splitting of water adsorbed on copper cluster ions followed by generation and escape of H_2 would be described by the reaction

$$(H_2O)_nCu_m^+ \rightarrow (H_2O)_{n-2}(OH)_2Cu_m^+ + H_2, \quad (1)$$

which could possibly be followed by the reaction

$$(H_2O)_{n-2}(OH)_2Cu_m^+ \rightarrow (H_2O)_{n-1}OCu_m^+. \quad (2)$$

A mass spectrum cannot distinguish between the reactant and product of reaction (2); the ion would commonly be identified as $(H_2O)_{n-1}OCu_m^+$. An even better indication of H_2 production would be the reaction

$$\begin{aligned}(H_2O)_nCu_m^+ &\rightarrow (H_2O)_{n-4}(OH)_4Cu_m^+ + 2H_2 \\ &\rightarrow (H_2O)_{n-2}O_2Cu_m^+ + 2H_2.\end{aligned} \quad (3)$$

Based on a DFT study of hydrated Cu_7, Stenlid et al. concluded that as many as 4 H_2 might be generated, which would result in $(H_2O)_{n-8}(OH)_8Cu_7$ or the isobaric $(H_2O)_{n-4}(O_2)_2Cu_7$ [16].

The theoretical studies of water dissociation on Cu_7 focus on neutral copper clusters [14–16] but Stenlid et al. [16] briefly mention Cu_7^- and Cu_7^+ as well. They point out that Cu_7^+ binds water more strongly, accommodates more water in the first solvation shell, and the Cu–Cu distances in the equatorial plane are increased relative to neutral Cu_7. It is not clear though to what degree the catalytic activities of Cu_7^+ and Cu_7 would differ.

We have searched for evidence of these types of water splitting reactions in our mass spectra, to no

avail. Unfortunately the sensitivity to the detection of $(H_2O)_{n-x}O_xCu_m^+$, $x \geq 1$ is hampered by two factors. First, these types of ions cannot be positively identified for even-numbered x in the mass range of interest ($\geq$63 + 32 u) because the mass of ions containing O_2 becomes indistinguishable from the mass of ions containing the contaminant PH. Second, the two naturally occuring isotopes of copper (^{63}Cu and ^{65}Cu, abundance 69.83% and 30.17%, respectively) produce highly congested spectra. The isotopologues are easily resolved up to, at least, Cu_{15}^+ (see the spectrum in Fig. 1a), but $O^{65}Cu^+$ and $H_2O^{63}Cu^+$ differ by only 0.018 u. The mass resolution of our instrument, $m/\Delta m \approx 3000$, is not quite sufficient to resolve these two ions; resolving them in complexes containing more than one copper atom would be a hopeless task. Experiments with isotopically enriched ^{63}Cu would alleviate this problem.

Theoretical studies pertain to neutral copper clusters containing 7 atoms while our work pertains to cationic clusters. Furthermore, the mass spectral resolution and the occurrence of isotopologues limits the information that we can deduce for ions containing more than a few copper atoms. Carnegie et al. have performed infrared photodissociation spectroscopy of argon-tagged H_2OCu^+ in the O–H stretching region [28]. Iino et al. have used a similar approach to study argon-tagged $(H_2O)_nCu^+$, $n \leq 4$, and untagged $(H_2O)_nCu^+$, $n \leq 7$ [27]. Their work provides no evidence for water splitting.

The catalytic activity of Cu_m^+ may be quite sensitive to its geometric and electronic structure, hence its size. In this context, the flagged feature in Figure 6b is noteworthy. It shows a greatly enhanced yield of dehydrogenated ions for just two species, $(H_2O)OHCu_2^+$ and $(H_2O)_2OHCu_2^+$. This suggests dissociative adsorption of H_2O on Cu_2^+ which would be a prerequisite for H_2 formation. Theoretical work is needed to elucidate the origin of this feature. Dehydrogenated hydrated copper ions have been characterized by collision-induced dissociation [32] and vibrational spectroscopy [29–31] but we are not aware of related work on ions containing two or more copper atoms.

The results presented in Figure 6 are markedly different from those reported earlier [19–33]. Michl and coworkers applied secondary-ion mass spectrometry of copper covered with a frozen water film [19]. The copper monomer formed a series of hydrated ions $(H_2O)_nCu^+$ but no dehydrogenated ions $(H_2O)_{n-1}OHCu^+$. The copper dimer formed the protonated series, the dehydrogenated series, and the doubly dehydrogenated series $(H_2O)_{n-1}OCu_2^+$, but no $(H_2O)_nCu_2^+$.

Stace and coworkers formed small copper cluster ions in an arc source; the ions were swept out by a helium carrier gas seeded with water vapor [33]. They detected only one complex containing a single copper atom, HCu^+. The hydrated copper dimer appeared in two forms, $(H_2O)_{n-1}HCu_2^+$ and $(H_2O)_{n-1}H_2Cu_2^+$. The hydrated copper trimer appeared in the protonated, dehydrogenated, and doubly dehydrogenated form but no $(H_2O)_nCu_3^+$ was observed. Thus, while we find that $(H_2O)_nCu_m^+$ is (with the exception of $m = 2$, $n = 2$ and 3) the most intense ion series, that series was not observed at all in previous work (with the exception of $(H_2O)_nCu^+$ [19]). Our tentative conjecture is that the very large excess energies that are available when ions are sputtered, or formed in a plasma, are responsible for the striking differences.

Finally we address the features marked in Figures 6a and 6c. The dissociation energy of $(H_2O)_2Cu^+$ is known to be about twice that of $(H_2O)_3Cu^+$; it is even higher than that of $(H_2O)Cu^+$ [18–20]. This rather unusual feature has been traced to the peculiar structure of $(H_2O)_2Cu^+$ whose lowest-energy structure has the H_2O molecules adsorbed on opposite sides of the Cu^+ ion with the O atoms facing Cu^+. Most theoretical studies agree that Cu^+ in $(H_2O)_3Cu^+$ and $(H_2O)_4Cu^+$ is two-fold coordinated, but the increase to three- or even four-fold coordination in ions containing as many 10 H_2O is less clear [21–25].

The local maximum in the abundance of $(H_2O)_nCu^+$ at $n = 2$ (see Fig. 5) signals its high stability. We also see an abrupt drop of the abundance at $(H_2O)_6Cu^+$ which suggests a sudden decrease in the dissociation energy. The only theoretical study of ions in this size range [25] reported relative energies of structural isomers relative to the ground state structure; dissociation energies of $(H_2O)_nCu^+$ ions in their ground state were not reported. However, it was noted that the coordination of Cu^+ increased from two or three for $n = 5$, 6 to three or four for $n \geq 7$. It is tempting to conjecture that this change in coordination is accompanied by a weakening in binding.

A pronounced local maximum occurs in the abundance distribution of the $(H_2O)_nCu_3^+$ series at $n = 3$. We are not aware of any studies of water adsorption on the copper trimer (nor trimers of other noble metals); theoretical work is needed to elucidate the origin of the apparent enhanced stability of $(H_2O)_3Cu_3^+$.

4.2 Copper–helium complexes

Figure 2 displays the abundance distributions of He_nCu^+ and $He_nCu_2^+$. Noteworthy are local maxima at $n = 6$, 12, and 24 in the He_nCu^+ series and an abrupt drop at $He_2Cu_2^+$; the features suggest enhanced stability of these ions. The high abundance of $He_{12}Cu^+$ might indicate icosahedral arrangement of the ligands, a structure observed for some other systems with non-directional bonding such as He_nK^+ [44], He_nAr^+ [45], He_nAg^+ [46], and He_nAu^+ [47]. Another factor in the appearance of icosahedral structure is that the size of the ion, i.e. the ion-ligand bond length, has to be about right for the size of the ligands, i.e. the ligand-ligand bond length. For He_nAr^+ the match is near-perfect, resulting in a highly ordered system with three distinct solvation shells of I_h symmetry [48].

For hard-sphere models, icosahedral packing is preferred if σ^*, the ratio of the ion-ligand and ligand-ligand lengths, lies between 0.82 and 0.95 [49]. Ab initio-calculations of the potential energy curves of He–Cu^+ result in bond lengths (R_e) of 1.93 or 1.95 Å [50,51]. The He–He bond length depends very much on the environment because of the large zero point energy. If one uses the helium bulk density for an estimate (which gives results in

reasonable agreement with dimer bond lengths for the heavier noble gases) one obtains $R_e \approx 2.52$ Å for He–He, and $\sigma^* \approx 0.77$. This value is midway between the range for which icosahedral packing would be favorable, and the range $0.61 \leq \sigma^* \leq 0.71$ for which octahedral packing would be favorable [49]. Thus the first two maxima in the abundance distribution in Figure 2, at $n = 6$ and 12, are not inconsistent with expectations based on hard-sphere packing models.

The only realistic theoretical study (at the coupled cluster single double triple level) of the stability of He_nCu^+ containing more than one helium atom was reported by Li et al. [52]; it extends to $n \leq 3$. The authors concluded that He_2Cu^+ is linear with D_∞ symmetry, and He_3Cu^+ is planar with D_{3h} symmetry. These features are not consistent with the assumption of non-directional bonding.

Another study worth mentioning is by Froudakis et al. [34]. The authors reported mass spectra of Ne_nCu^+ and Ar_nCu^+. The abundance distribution of Ne_nCu^+ suggested enhanced stability at $n = 4$ and 12; DFT calculations confirmed this conjecture. The ground state structure of $Ne_{12}Cu^+$ turned out to be icosahedral even though for Ne–Cu^+ the value of σ^* is only ≈0.66, within the range where hard-sphere packing models would favor octahedral packing. Ne_6Cu^+ had the largest computed dissociation energy in the size range $3 \leq n \leq 13$; its structure was a strongly distorted octahedron of C_{2v} symmetry.

To summarize, local abundance maxima at He_6Cu^+ and $He_{12}Cu^+$ have been tentatively assigned to octahedral and icosahedral structures; calculations are needed to confirm this conjecture. Existing theoretical reports of small He_nCu^+ and larger Ne_nCu^+ indicate that He_nCu^+ cannot be modeled by simple pairwise additive potentials. We have made no attempt to provide structural models for $He_{24}Cu^+$ and $He_2Cu_2{}^+$ which also seem to enjoy enhanced stability.

5 Conclusion

We have attempted to detect evidence for the production and release of H_2 from cationic copper-water complexes in the gas phase. The reaction would have to proceed after (or upon) ionization because of the low temperature of the helium droplets in which the neutral precursors are grown. We failed to detect the telltale of H_2 production, i.e. ions of the composition $(H_2O)_{n-2}(OH)_2Cu_m{}^+$ or the isobaric $(H_2O)_{n-1}OCu_m{}^+$ (or $(H_2O)_{n-2}O_2Cu_m{}^+$ which would indicate the production of 2 H_2). In future work we plan to use isotopically enriched copper; this would greatly reduce the number of isotopologues for ions containing several copper atoms, and increase the sensitivity for the detection of $(H_2O)_{n-x}O_xCu_m{}^+$.

We did detect ions that suggest highly size-dependent reactions, namely very intense signals for $(H_2O)OHCu_2{}^+$ and $(H_2O)_2OHCu_2{}^+$; the latter forms a maximum in the $(H_2O)_nOHCu_2{}^+$ series and exceeds the abundance of $(H_2O)_3Cu_2{}^+$.

Another interesting observation is the large abundance of He_6Cu^+, $He_{12}Cu^+$, $He_{24}Cu^+$, and $He_2Cu_2{}^+$. It is tempting to speculate that the apparently high stability of the first two of these ions correlates with octahedral and icosahedral arrangements of the solvent atoms. Theoretical work is needed to confirm these conjectures, and to provide a rational for the postulated enhanced stability of $He_{24}Cu^+$ and He_2Cu_2.

This work was given financial support by the Austrian Science Fund (FWF) Wien (Project P26635) and the European Commission (ELEVATE, Horizon 2020 research and innovation program under grant agreement No. 692335). Open access funding provided by Institut für Ionenphysik und Angewandte Physik.

Author contribution statement

P. Scheier conceived the project; S. Raggl, N. Gitzl, and P. Martini carried out the experimental work and data analysis; O. Echt prepared a draft of the manuscript; all authors discussed the results and commented on the manuscript.

References

1. Z.X. Yang, L.G. Xie, D.W. Ma, G.T. Wang, J. Phys. Chem. C **115**, 6730 (2011)
2. J. Xiong, X.D. Wu, Q.J. Xue, J. Colloid Interface Sci. **390**, 41 (2013)
3. N.K. Das, S. Ghosh, A. Priya, S. Datta, S. Mukherjee, J. Phys. Chem. C **119**, 24657 (2015)
4. T. Kruk, K. Szczepanowicz, J. Stefanska, R.P. Socha, P. Warszynski, Colloids Surf. B-Biointerfaces **128**, 17 (2015)
5. Z.K. He, J.W. Fu, B. Cheng, J.G. Yu, S.W. Cao, Appl. Catal. B-Environ. **205**, 104 (2017)
6. Y.P. Liu et al., Adv. Mater. **29** (2017)
7. G. Hultquist, M.J. Graham, O. Kodra, S. Moisa, R. Liu, U. Bexell, J.L. Smialek, Corros. Sci. **95**, 162 (2015)
8. A.J. Johansson, C. Lilja, T. Brinck, J. Chem. Phys. **135**, 084709 (2011)
9. C.M. Lousada, A.J. Johansson, P.A. Korzhavyi, J. Phys. Chem. C **119**, 14102 (2015)
10. K. Andersson, G. Ketteler, H. Bluhm, S. Yamamoto, H. Ogasawara, L.G.M. Pettersson, M. Salmeron, A. Nilsson, J. Am. Chem. Soc. **130**, 2793 (2008)
11. P. Kappen, J.D. Grunwaldt, B.S. Hammershoi, L. Troger, B.S. Clausen, J. Catal. **198**, 56 (2001)
12. M. Estrella et al., J. Phys. Chem. C **113**, 14411 (2009)
13. S. Huseyinova, J. Blanco, F.G. Requejo, J.M. Ramallo-Lopez, M.C. Blanco, D. Buceta, M.A. Lopez-Quintela, J. Phys. Chem. C **120**, 15902 (2016)
14. L. Chen et al., Phys. Chem. Chem. Phys. **12**, 9845 (2010)
15. J.H. Stenlid, A.J. Johansson, T. Brinck, Phys. Chem. Chem. Phys. **16**, 2452 (2014)

16. J.H. Stenlid, A.J. Johansson, L. Kloo, T. Brinck, J. Phys. Chem. C **120**, 1977 (2016)
17. M.L. Jiang, Q. Zeng, T.T. Zhang, M.L. Yang, K.A. Jackson, J. Chem. Phys. **136**, 104501 (2012)
18. P.M. Holland, A.W. Castleman, J. Chem. Phys. **76**, 4195 (1982)
19. T.F. Magnera, D.E. David, D. Stulik, R.G. Orth, H.T. Jonkman, J. Michl, J. Am. Chem. Soc. **111**, 5036 (1989)
20. N.F. Dalleska, K. Honma, L.S. Sunderlin, P.B. Armentrout, J. Am. Chem. Soc. **116**, 3519 (1994)
21. P.J.E. Boussard, P.E.M. Siegbahn, M. Svensson, Chem. Phys. Lett. **231**, 337 (1994)
22. A.M. El-Nahas, N. Tajima, K. Hirao, J. Mol. Struct. THEOCHEM **469**, 201 (1999)
23. D. Feller, E.D. Glendening, W.A. de Jong, J. Chem. Phys. **110**, 1475 (1999)
24. H.M. Lee, S.K. Min, E.C. Lee, J.H. Min, S. Odde, K.S. Kim, J. Chem. Phys. **122**, 064314 (2005)
25. J.D. Herr, R.P. Steele, J. Phys. Chem. A **120**, 10252 (2016)
26. T. Iino, K. Ohashi, Y. Mune, Y. Inokuchi, K. Judai, N. Nishi, H. Sekiya, Chem. Phys. Lett. **427**, 24 (2006)
27. T. Iino, K. Ohashi, K. Inoue, K. Judai, N. Nishi, H. Sekiya, J. Chem. Phys. **126**, 194302 (2007)
28. P.D. Carnegie, A.B. McCoy, M.A. Duncan, J. Phys. Chem. A **113**, 4849 (2009)
29. B.M. Marsh, J. Zhou, E. Garand, J. Phys. Chem. A **118**, 2063 (2014)
30. B.M. Marsh, J. Zhou, E. Garand, Phys. Chem. Chem. Phys. **17**, 25786 (2015)
31. A.F. Sweeney, J.T. O'Brien, E.R. Williams, P.B. Armentrout, Int. J. Mass Spectrom. **378**, 270 (2015)
32. A.F. Sweeney, P.B. Armentrout, J. Phys. Chem. A **118**, 10210 (2014)
33. V.A. Mikhailov, P.E. Barran, A.J. Stace, Phys. Chem. Chem. Phys. **1**, 3461 (1999)
34. G.E. Froudakis, M. Muhlhauser, S.C. Farantos, A. Sfounis, M. Velegrakis, Chem. Phys. **280**, 43 (2002)
35. L.F. Gomez, E. Loginov, R. Sliter, A.F. Vilesov, J. Chem. Phys. **135**, 154201 (2011)
36. H. Schöbel, P. Bartl, C. Leidlmair, S. Denifl, O. Echt, T.D. Märk, P. Scheier, Eur. Phys. J. D **63**, 209 (2011)
37. S. Ralser, J. Postler, M. Harnisch, A.M. Ellis, P. Scheier, Int. J. Mass Spectrom. **379**, 194 (2015)
38. A. Mauracher, M. Daxner, J. Postler, S.E. Huber, S. Denifl, P. Scheier, J.P. Toennies, J. Phys. Chem. Lett. **5**, 2444 (2014)
39. O. Echt, D. Kreisle, M. Knapp, E. Recknagel, Chem. Phys. Lett. **108**, 401 (1984)
40. S. Denifl et al., J. Chem. Phys. **132**, 234307 (2010)
41. S. Krückeberg, L. Schweikhard, J. Ziegler, G. Dietrich, K. Lutzenkirchen, C. Walther, J. Chem. Phys. **114**, 2955 (2001)
42. C.E. Klots et al., Z. Phys. D **21**, 335 (1991)
43. K. Hansen, U. Näher, Phys. Rev. A **60**, 1240 (1999)
44. L. An der Lan, P. Bartl, C. Leidlmair, R. Jochum, S. Denifl, O. Echt, P. Scheier, Chem. Eur. J. **18**, 4411 (2012)
45. P. Bartl, C. Leidlmair, S. Denifl, P. Scheier, O. Echt, J. Phys. Chem. A **118**, 8050 (2014)
46. T. Döppner, T. Diederich, S. Gode, A. Przystawik, J. Tiggesbäumker, K.H. Meiwes-Broer, J. Chem. Phys. **126**, 244513 (2007)
47. M. Goulart et al., Phys. Chem. Chem. Phys. **20**, 9554 (2018)
48. F. Tramonto, P. Salvestrini, M. Nava, D.E. Galli, J. Low Temp. Phys. **180**, 29 (2015)
49. D. Prekas, C. Lüder, M. Velegrakis, J. Chem. Phys. **108**, 4450 (1998)
50. A. Yousef, S. Shrestha, L.A. Viehland, E.P.F. Lee, B.R. Gray, V.L. Ayles, T.G. Wright, W.H. Breckenridge, J. Chem. Phys. **127**, 154309 (2007)
51. X.F. Tong, C.L. Yang, M.S. Wang, X.G. Ma, D.H. Wang, J. Chem. Phys. **134**, 024306 (2011)
52. X.Y. Li, X.Y. Cheng, X. Cao, Struct. Chem. **23**, 1831 (2012)